Mechanical Systems and Signal Processing 175 (2022) 109135

Contents lists available at ScienceDirect

Mechanical Systems and Signal Processing

journal homepage: www.elsevier.com/locate/ymssp

# Fidelity assessment of Real-Time Hybrid Substructuring based on convergence and extrapolation

Christina Insam *, Daniel J. Rixen

*Technical University of Munich, School of Engineering & Design, Department of Mechanical Engineering, Chair of Applied Mechanics, Boltzmannstr. 15, 85748 Garching, Germany*
*Technical University of Munich, Munich Institute of Robotics and Machine Intelligence (MIRMI), Germany*

ARTICLE INFO

Communicated by J. Baqersad

Dataset link: https://gitlab.lrz.de/AM/rths

*Keywords:*
Real-Time Hybrid Substructuring
Real-time hybrid simulation
Hardware-in-the-loop testing
Fidelity assessment
Accuracy measure

ABSTRACT

High quality of products and quick development cycles require reliable verification of the products. An applicable method for component testing is Real-Time Hybrid Substructuring (RTHS), which is a cyber–physical testing method combining numerical simulation and experimental testing. For the broad application of such testing methods, confidence in the test results must be gained. For this purpose, fidelity measures are required to indicate to the user how trustworthy the results are. The fidelity of an RTHS test does not only depend on the amount of errors in the loop, but also on the dynamics of the reference system and the interface locations. Current assessment measures do either not consider these dynamics/partitioning or require a reference solution or need knowledge about the dynamics of all involved components. This work proposes a novel strategy for fidelity assessment that circumvents these shortcomings: Fidelity Assessment based on Convergence and Extrapolation (FACE). The main idea is to deliberately vary the amount of error in the RTHS loop and monitor how this changes the RTHS result. From this relation, system understanding can be gained that is used in a further step to estimate the dynamics of the reference solution (i.e., if there was no error in the loop). The proposed method is applied to two application examples. In the first example, which is a virtual RTHS test of a linear system, the true reference solution is available and the prediction capability of the FACE method is verified. The second example uses data from a real RTHS test. Both examples reveal that the FACE method captures the dynamics influence of an error on the RTHS result and therefore helps the user to decide whether the conducted test was successful. This method can therefore be a valuable tool to assist users in the application of RTHS to a large variety of systems.

## 1. Introduction

Real-Time Hybrid Substructuring (RTHS) is a cyber–physical testing method where numerical simulation and experimental testing are combined. This setup combines the advantages of both testing methods: parts that are dynamically well understood, not yet available as hardware, too large to be tested experimentally or where the influence of varying dynamic properties should be analyzed are modeled in the numerical substructure. In turn, critical components, parts that potentially fail during operation or components/phenomena that are difficult to model are tested experimentally [1]. The substructures are coupled in real-time at a fixed sampling rate $\delta t$ using actuation, sensing and a Digital Signal Processor (DSP). Over the last two decades, RTHS has been applied to a variety of applications ranging from civil engineering to aerospace and mechanical engineering as well as robotics [2–4].

* Corresponding author.
*E-mail addresses:* christina.insam@tum.de (C. Insam), rixen@tum.de (D.J. Rixen).

https://doi.org/10.1016/j.ymssp.2022.109135
Received 14 December 2021; Received in revised form 24 March 2022; Accepted 6 April 2022
Available online 20 April 2022

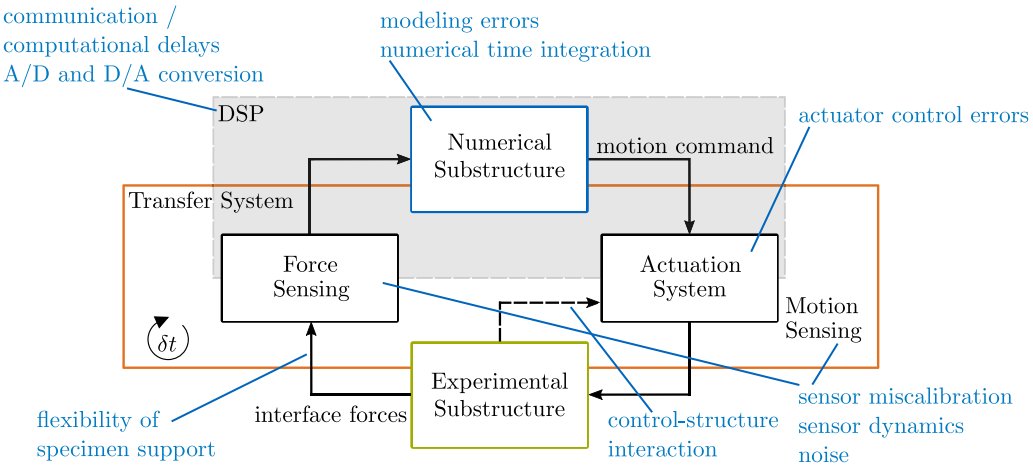


**Fig. 1.** Coupling of numerical and experimental substructures in RTHS is done in real-time by the transfer system, which comprises the actuation system, sensing and a DSP. The most relevant error sources in the RTHS loop are shown in this figure.

There are several challenges associated with RTHS testing, which prevent the method from being even more widely used and accepted. One of them is the fidelity assessment: There are several sources of systematic and random errors in the RTHS loop [5–8].

**Errors:** distort the dynamics of an RTHS test from the reference dynamics and can originate from the numerical substructure or the physical components. They are visualized in Fig. 1.

Due to the feedback structure of the RTHS loop, errors are propagated through the loop over the whole time history of the RTHS test. This leads to a distortion of the test results compared to the reference dynamics [9].

**Reference dynamics:** refers to the real dynamic behavior of the overall system, viz. when the analyzed dynamical system is operated in its final application. The reference dynamics result in an RTHS test when there are no errors (perfect modeling of the numerical part, synchronization of substructures, ...).

**Success of an RTHS test:** is given if the "[...] RTHS system captures the essential dynamics of the reference system [...]" [8] and **fidelity** is defined as "[...] the degree to which it reproduces the behavior of the real system under study." [10]

Since errors are inevitable, fidelity measures are necessary to determine whether the RTHS results can be trusted and to gain confidence in the test. Setting up such fidelity measures is not trivial because the susceptibility of an RTHS setup to a certain amount of error depends on the reference dynamics (e.g., eigenfrequency or damping), the partitioning into numerical and experimental substructure, and the objective of the test [8,11,12]. A long-term goal of the RTHS community is to set up acceptance criteria that classify the performance of an RTHS test into accepted (reference dynamics sufficiently replicated) and failed [12]. Due to the involved complexity of fidelity assessment, this goal has not yet been achieved despite great progress in the understanding of error sources, test stability, etc.

This work aims at proposing a novel approach for fidelity assessment of RTHS tests. The approach is called Fidelity Assessment based on Convergence and Extrapolation (FACE) and is characterized by a simple implementation that can be applied to a large range of dynamical systems, only uses data that are available during the test and does not require a reference solution.

An overview about state-of-the-art accuracy measures is given in Section 2 and their advantages and shortcomings are summarized. Section 3 presents the FACE method, which is applied to two application examples in Section 4. In that section, we also critically discuss the different aspects of the proposed strategy. This article is concluded by a summary in Section 5.

## 2. State-of-the-Art

This section should give a brief overview about currently existing accuracy measures and research directions in this field. More extensive reviews can be found in [11,12].

The term *accuracy measures* encompasses all measures that evaluate the RTHS test performance. This means that they also include measures of the amount of error, such as for example the tracking accuracy or other local measures of the interface synchronization. As mentioned previously, the success of an RTHS test does not only depend on the amount of these errors, but also on the test susceptibility. All measures that relate the test result to a reference solution and all measures that capture the impact of errors in a global sense are henceforth called *fidelity measures*.

Following [8], accuracy measures can be classified into pre-test, online and post-test measures. Pre-test measures indicate the requirements on the actuator performance and evaluate the test susceptibility. For example, the predictive stability/performance

indicators proposed in [13] help to select the best partitioning (if one has the choice) of the dynamical system to reduce the test susceptibility to errors. Using online indicators, an ongoing test can be monitored and interrupted if there are noticeable errors or if the experimental part/transfer system could be damaged [14,15]. The test fidelity is assessed using post-test measures by comparing the RTHS test results to a reference solution (in time or frequency domain) or by evaluating the data (e.g., interface desynchronization).

To evaluate the interface synchronization, the actuator tracking performance can be analyzed. One option is to build the relative root-mean-square (RMS) tracking error

$$e_{\text{track,RMS}} = \frac{RMS(z - z')}{RMS(z)}, \tag{1}$$

where the commanded actuator motion is $z$ and the achieved actuator motion is $z'$. The tracking performance can also be visualized in the Synchronization Subspace Plot [16], where $z$ is plotted against $z'$, or using the Frequency Evaluation Index [17,18], which evaluates the actuator delay and amplitude error. The interface synchronization can furthermore be quantified by monitoring the energy/power flow at the interface, which means evaluating how much energy is generated/dissipated by the transfer system at the interface [14,19,20]. The limitation of these measures is that they do only quantify the error, but do not tell the influence of this error on the distortion of the reference dynamics because they do not include the partitioning or dynamics of the reference system. Hence, no general rule for an appropriate threshold value can be given.

Pre-test approaches that consider this effect are the predictive performance indicator by Maghareh et al. [8,13] and the condition of robust performance by Botelho and Christenson [21,22]. Surrogate modeling of the coupled system including uncertainties of dynamical system properties and errors is a further research direction [5,23–25]. These pre-test indicators require that the dynamics of the involved components (transfer system and/or experimental part) are known or at least in an approximated way.

To sum up, currently applied accuracy measures are not sufficient to assess the success of an RTHS test and further research is required. Novel fidelity measures should

- capture the effect of an error on the observed dynamics in the RTHS test
- measure the fidelity (i.e., relate the RTHS result to the reference dynamics)
- not require a reference solution or system identification of the involved parts
- be applicable to a large variety of dynamical systems for different sources of errors
- have a straightforward implementation
- be easy to understand

## 3. Fidelity assessment based on convergence and extrapolation (FACE)

No matter how carefully an RTHS test is conducted, there are always errors. In most of the cases the severity of these errors can be quantified with an error measure $e$. When an RTHS test is conducted, usually the best error mitigation and the best of the implemented actuator control schemes are selected. This leads to the minimum achievable error $e_{\text{min}}$. The underlying idea of the proposed strategy is to vary the error and see how this affects a measure of the RTHS result $q$. The error can be increased up to the stability limit $e_{\text{crit}}$, above which the RTHS test is unstable. Within $e_{\text{min}} \leq e < e_{\text{crit}}$ (explorable area), the error can be deliberately altered and the influence on the RTHS result $q$ monitored. If all errors are quantified within the error measure $e$, the reference dynamics result in case $e = 0$. The measurement points within the explorable area can be used to find a relation $q = h(e)$ to predict the value of $q$ at $e = 0$, which is an estimate $q_{\text{pred}}$ of the true reference dynamics $\hat{q}$. If $e_{\text{min}}$ is in the linear regime, which means that the overall dynamics do not substantially change between $0 < e < e_{\text{min}}$, and $h(e)$ is accurately identified, then the prediction is close to the true reference solution, that is $q_{\text{pred}} \approx \hat{q}$. The fidelity of the performed test (RTHS result $q_{\text{min}}$) can be compared to $q_{\text{pred}}$ and a decision taken whether the test succeeded. Hence, this method performs a fidelity assessment based on convergence and extrapolation, which is abbreviated as FACE henceforth. The basic principle is illustrated in Fig. 2.

The measures of the error $e$ and the RTHS result $q$ must be scalars and their specific choice depends on the main error source(s) and the objective of the test. Examples for $e$ include the accuracy measures (cf. Section 2 or see [11,12]) or a combination of them. The requirement is that the RTHS results converge to the reference dynamics as $e \to 0$. If there are known and significant errors that are not quantified within $e$, the FACE method can only be used as a tool for experimental sensitivity analysis to investigate the susceptibility of an RTHS setup to a certain error source. Even though these results cannot be used further for quantitative evaluation of the test fidelity, the results of such an experimental sensitivity analysis can be valuable to understand the influence of an error on the test results. The RTHS result $q$ denotes the Quantity of Interest (QoI) of an RTHS test, which can be any physical quantity of the coupled dynamical system [25]. To name a few examples, the oscillation frequencies of the structure, the displacement magnitude, the maximum stress or the peak interface force could be appropriate QoIs. If there are multiple QoIs for one RTHS test, the convergence plot Fig. 2 can be plotted and analyzed for each QoI individually (cf. [26]).

There are several requirements on the interpolation function $h(e)$. The sign of the curvature must not change in the extrapolated region. This is because we assume that the general trend is captured by $h(e)$ and that $e_{\text{min}}$ is sufficiently small such that the overall dynamic behavior of the RTHS test does not change for $e \in [0, e_{\text{min}}]$. The degree of the polynomial used for interpolation must be smaller than the number of measurement points and overfitting should be avoided. In our experience, polynomials of degree two, three or four were sufficient to capture the essential dynamics, i.e. the general trend. Apart from polynomials, also spline functions might be used to fit $h(e)$. The specific choice of the interpolation functions $h(e)$ for the application examples is explained later.

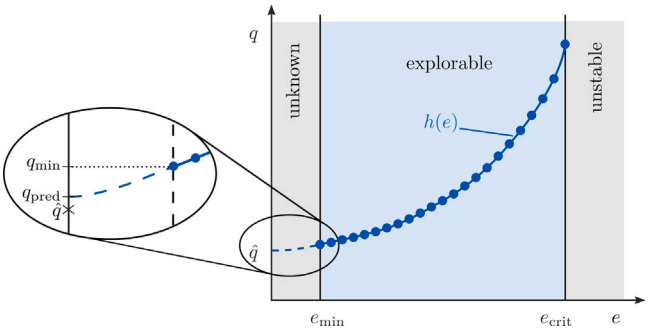


**Fig. 2.** The basic idea of FACE: a convergence plot is generated by deliberately changing the amount of error $e$ in the RTHS setup and monitoring the RTHS result $q$. Using the measurement points, the function $h(e)$ can be determined and used to extrapolate to $e = 0$. The result $q_{\text{min}}$ at $e_{\text{min}}$ can then be compared to $q_{\text{pred}} \approx \hat{q}$ and the fidelity inferred.

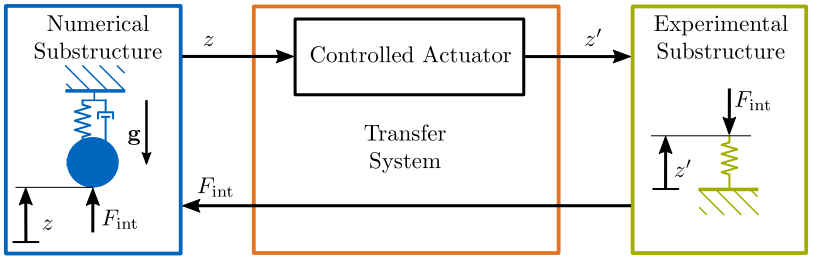


**Fig. 3.** The coupled linear system used for the vRTHS tests. As actuator dynamics and control, a model of an electric actuator has been taken [28].

## 4. Example applications

The FACE method has been applied to different example applications, where two of them are presented in this section. Firstly, the efficiency of the method is validated using a virtual RTHS (vRTHS) test. This example is used because a reference solution is available and therefore the prediction capability of FACE can be investigated. The second example is an RTHS shock test that uses data from a real RTHS test [27]. This section concludes with a discussion of the advantages and shortcomings of the proposed method.

### 4.1. Example 1: Virtual RTHS test

The dynamical system and the associated RTHS setup are depicted in Fig. 3. A mass–spring–damper system is modeled numerically and interacts with a linear spring in the experimental substructure. The simulated load case considers an external force that balances the gravity force on the mass such that both springs are undeformed for $t < 0\,\text{s}$. At time $t = 0\,\text{s}$, the external force is removed and the coupled mass–spring–damper oscillates with its eigenfrequency

$$\omega_{\text{dyn}} = \sqrt{\frac{k_{\text{NUM}} + k_{\text{EXP}}}{m_{\text{NUM}}} - \left(\frac{d_{\text{NUM}}}{2 \cdot m_{\text{NUM}}}\right)^2}, \tag{2}$$

where $k_{\text{NUM}}$ and $k_{\text{EXP}}$ are the stiffness of the numerical and experimental part, $m_{\text{NUM}}$ is the mass of the numerical substructure and $d_{\text{NUM}}$ its damping. Due to the damping, the system comes at rest at the deflected position $z = -\frac{m_{\text{NUM}} \cdot g}{k_{\text{NUM}} + k_{\text{EXP}}}$. The transfer system is modeled as follows: The dynamics of the DSP and the sensors are assumed to be ideal and a model of an electric actuator is implemented. The dynamics of the actuator are measured transfer functions from command voltage to actuator stroke of an actuator that exists at the Technical University of Munich. The implemented control scheme is a cascaded controller, which consists of an inner velocity control loop and an outer position control loop (proportional gain $K_{\text{P}}$) [28].

In this modeled setup, the tracking performance of the actuator is the only error source. The best actuator tracking performance ($e_{\text{min}}$) is achieved with a proportional gain of $K_{\text{P}} = 90\,1/\text{s}$ in the position control loop. The selected dynamical system parameters were $m_{\text{NUM}} = 9.62\,\text{kg}$, $k_{\text{NUM}} = 2 \cdot 10^4\,\text{N/m}$, $d_{\text{NUM}} = 200\,\text{Ns/m}$ and $k_{\text{EXP}} = 8650\,\text{N/m}$ and the sample time was $\delta t = 0.001\,\text{s}$. To investigate how the dynamics of the RTHS test are affected by the actuator dynamics, FACE was applied. For this dynamical system, the oscillation behavior is of particular interest and the three QoIs are the oscillation amplitude $a$, the system damping $d$ and the vibration frequency $f$. The error in this vRTHS setup comes from the limited actuator performance. Hence, one possible choice for the error measure $e$ is the relative RMS tracking error $e_{\text{track,RMS}}$ from Eq. (1). To apply the FACE method, the error has to be deliberately altered.

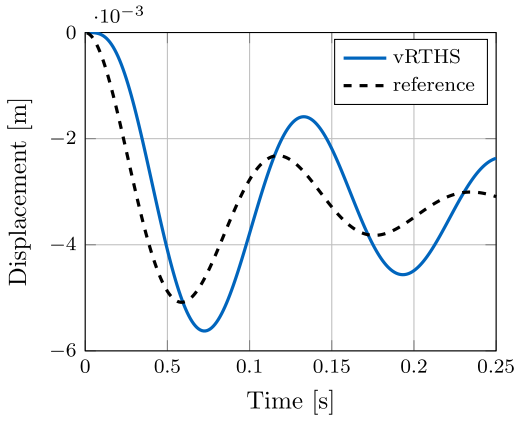


(a) Interface displacement of the vRTHS test (blue, solid) and the reference solution (black, dashed).

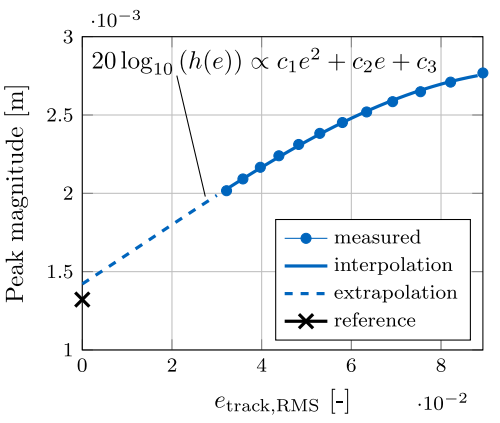


(b) Measurement points of the FACE method using artificial delay $\tau_{\text{add}}$.

**Fig. 4.** To investigate the impact of actuator delay on the oscillation magnitude, artificial delay $\tau_{\text{add}}$ is inserted into the loop and the peak magnitude $a = max(FFT(z'))$ is monitored. The measurement points are indicated by blue dots, where the left-most dot corresponds to $e_{\text{min}}$ (i.e., no additional $\tau_{\text{add}}$). The measurement points are used for a polynomial interpolation (solid line) of degree two with coefficients $c_1$, $c_2$ and $c_3$ to find $h(e)$, which in turn is used to extrapolate to $e_{\text{track,RMS}} = 0$. The amplitude of the reference solution $\hat{a}$ is indicated by the black cross.

As the experimental part only contains stiffness, the actuator delay has a destabilizing effect, which is an effect like negative damping [29,30]. This directly leads to larger oscillation amplitudes. When the FACE method is applied for the QoIs $a$ and $d$, artificial delay $\tau_{\text{add}}$ can be added to see how this influences the RTHS results, which is how detrimental the effect of $\tau_{\text{add}}$ is for this specific setup. $\tau_{\text{add}}$ was used to delay the motion command $z$ that is sent to the actuator and the specific implemented values[1] were $\tau_{\text{add}} = \{0.001, 0.002, \dots, 0.011\}$ s. First, the oscillation amplitude was examined. A tool to quantify the oscillation amplitude with a scalar value is the Fourier transform. This amplitude value can be better interpreted for steady-state oscillations. Since the oscillation amplitude decreases in the investigated system due to damping, the Fourier transform was only applied to the first 0.25 s of the signal $z'$. Fig. 4(a) shows the time course of the oscillation during the vRTHS test (without additional $\tau_{\text{add}}$) and the reference solution, which is the intended but usually unknown behavior. For each value $\tau_{\text{add}}$, a vRTHS simulation was conducted and the measured displacement $z'$ recorded. Then, the Fourier transform of the first 0.25 s of the signals was performed and the peak magnitudes $a$ extracted and plotted against the corresponding $e_{\text{track,RMS}}$ in Fig. 4(b). The measurement points were then used to find the relation $q = h(e)$, specifically $a = h(e_{\text{track,RMS}})$. Investigations in [26] showed that the functional course of the measurement points resembles an exponential function.[2] To fit an exponential function, the base and the exponents have to be found. This can be done by transforming the measurement values logarithmically, for example with $a[dB] = 20 \cdot \log_{10}\left(\frac{a[m]}{1[m]}\right)$ and fitting a polynomial to the transformed values. Here, a polynomial of degree two was used for interpolation/extrapolation because this fulfills the following conditions: (i) it achieved the best function fit (least error compared to polynomials of degree one, three or four) (ii) the sign of the curvature does not change in the extrapolated area $e \in [0, e_{\text{min}}]$. Using the polynomial, the estimated reference solution of the magnitude is $a_{\text{pred}} = 1.42 \cdot 10^{-3}$ m compared to the true value of the reference solution $\hat{a} = 1.32 \cdot 10^{-3}$ m. This makes a relative prediction error of $\frac{a_{\text{pred}} - \hat{a}}{\hat{a}} = 0.075$. Comparing $a_{\text{pred}}$ with the results of the vRTHS test without additional delay $a_{\text{min}} = 2.017 \cdot 10^{-3}$ m, the error of the vRTHS can be estimated. The relative error of the vRTHS test is $\frac{a_{\text{min}} - a_{\text{pred}}}{a_{\text{pred}}} = 0.295$, which is quite large. Using these values one can conclude that the vRTHS test was not successful if the replication of the amplitude behavior is of critical importance.

Using the same measurements, also the effective damping can be investigated.[3] The damping constant was found for each test using a function fit for the envelope of the decaying oscillations.[4] The values are plotted in Fig. 5(a). To interpolate the course of these measurement points, a polynomial of degree four proved applicable (good fit of measurement points, sign of curvature does not change in the extrapolated region). The predicted damping constant is $d_{\text{pred}} = 185.2$ Ns/m, which yields a relative prediction error of $\frac{\hat{d} - d_{\text{pred}}}{\hat{d}} = 0.074$ compared to the true damping of $\hat{d} = d_{\text{NUM}} = 200$ Ns/m. Comparing the damping $d_{\text{min}} = 95$ Ns/m to the predicted solution (or the true reference), one can see that the effective damping is significantly modified due to the actuator dynamics.

Finally, the effect of uncompensated actuator dynamics on the oscillation frequency $f$ in the vRTHS test is considered to determine whether the frequency content is replicated correctly in the test. To alter the frequency content that is visible in the

[1] The selected values of $\tau_{\text{add}}$ were all within the explorable area and well below the stability limit. They are multiples of $\delta t$.

[2] The investigations in [26] also revealed that fitting with an exponential function is more accurate than fitting with a polynomial.

[3] Note that in this system, the damping of the coupled system is known, as there is only damping in the numerical substructure. In general, however, there is also damping in the experimental part, which is unknown.

[4] The damping values could have also been retrieved from the sharpness of the resonance in the magnitude frequency response.

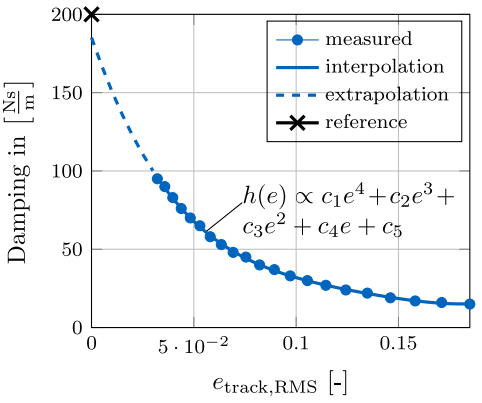


(a) FACE is applied to predict the overall system damping. The error $e_{\text{track,RMS}}$ was varied using additional delay $\tau_{\text{add}}$.

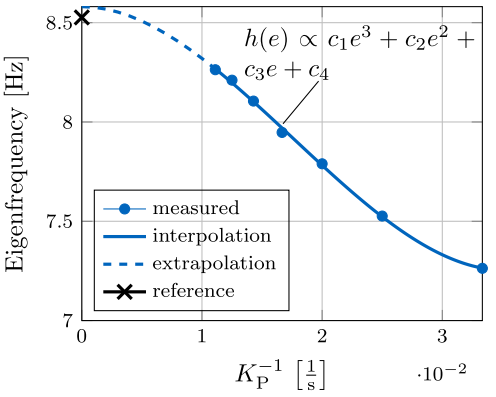


(b) The eigenfrequency visible in the vRTHS test changes depending on the actuator bandwidth. Different values of $K_{\text{P}}$ lead to different measurement points.

**Fig. 5.** The FACE method is applied to predict the overall system damping and the eigenfrequency of the coupled dynamical system.

vRTHS test, the bandwidth of the controlled actuator is changed. This is done by varying the controller parameter $K_{\text{P}}$. In general, the controller bandwidth increases for higher $K_{\text{P}}$ and decreases for lower $K_{\text{P}}$ [31]. $K_{\text{P}}$ must remain under a certain limit to ensure stability of the controlled actuator. The selected controller parameters were $K_{\text{P}} = \{20, 30, \ldots, 90\}$ 1/s, where the worst tracking behavior is expected for $K_{\text{P}} = 20$ 1/s. Also $e_{\text{track,RMS}}$ could be used as above as error measure. To showcase a different choice, $K_{\text{P}}^{-1}$ is used in this case as quantity on the abscissa. This is an appropriate choice because it is a scalar value that approaches zero for perfect actuator tracking, which is when $K_{\text{P}} \to \infty$. The results are shown in Fig. 5(b). Due to the limited actuator performance and low actuator bandwidth, the frequency content that was visible in the vRTHS test is lower than the true eigenfrequency. This means that the actuator acted like a filter on the frequency content that is transferred between the numerical and the experimental part for this setup.[5] The higher the actuator bandwidth, the closer the frequency content of the vRTHS test is to the reference eigenfrequency $\hat{f}$. The measurement points were fitted using a polynomial of degree three. This polynomial was selected because it yields a good fit of the measurement points and the sign of the curvature does not change in the extrapolated region. Furthermore, the gradient approaches zero as $e \to 0$, which is an additional condition for the extrapolation of the eigenfrequency that is based on the investigations in [26]. Using a polynomial of degree three, the predicted eigenfrequency is very close to the true eigenfrequency: $f_{\text{pred}} = 8.58$ Hz and $\hat{f} = 8.53$ Hz. The eigenfrequency using the highest value of $K_{\text{P}}$ is $f_{\text{min}} = 8.26$ Hz, which is quite close to the predicted/reference eigenfrequency and these results can be trusted.

### 4.2. Example 2: RTHS shock testing

This second example shows the application of the FACE method to the experimental data of an RTHS shock test. The system is depicted in Fig. 6. Here, a hammer is mounted with a pivot joint and locked at an initial angle $\Theta_0$ by a locking mechanism. When the locking is released, the hammer swings down and strikes a mass–spring–damper system. Since modeling the impact phenomenon between the contact partners is challenging, it is part of the experimental substructure. The objective of this RTHS test is to study the interaction force for varying parameters of the mass–spring–damper system. To change them easily, the mass–spring–damper system is modeled numerically. An electrodynamic shaker is used as actuation system and an impedance sensor is mounted at the tip of the shaker to measure the interaction force $F_{\text{int}}$ for the RTHS coupling and the shaker accelerations for control. The shaker is controlled using an acceleration control loop. This means that the motion command by the numerical substructure is $\ddot{z}$. The shaker is controlled using a combination of a minimum phase inverse compensator (MPIC) and Iterative Learning Control (ILC). MPIC is a model-based compensator that uses an inverted model of the shaker dynamics for compensation. In ILC, several trials (here: RTHS tests) are performed and this scheme learns an appropriate feedforward signal for the shaker to reduce the tracking error from iteration to iteration. In this work, two different learning functions were implemented in ILC: firstly, a proportional learning function (PILC) was used and secondly a model-based learning function (MBILC) [32]. The proportional learning function converges slower and has a higher remaining error, but does not require model knowledge. The model-based learning function uses an inverted model of the electrodynamic shaker and achieves smaller remaining errors and faster convergence if the model is accurate. This test setup is presented in detail in [27] and the application of ILC to RTHS tests was proposed in [33].

The system parameters of the mass–spring–damper system were tuned such that the numerical mass had the same weight as the hammer, the eigenfrequency was 100 Hz and the system damping was 5 %. The initial angle of the pendulum was $\Theta_0 = 15°$. Also, in this setup, the main error comes from the limited tracking performance of the electrodynamic shaker: the shaker needs to

[5] Note that this statement is only true for stiffness experimental parts, cf. [26].

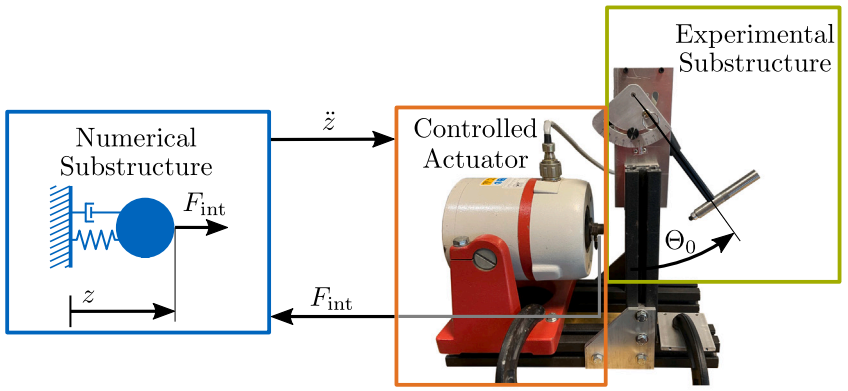


**Fig. 6.** A hammer mounted with a pivot joint swings (experimental part) and hits a mass–spring–damper system (numerical substructure). An electrodynamic shaker performs the motion command of the numerical substructure $\ddot{z}$ and an impedance sensor measures the interaction forces $F_{\text{int}}$. A performance real-time target machine is used as DSP (not depicted).

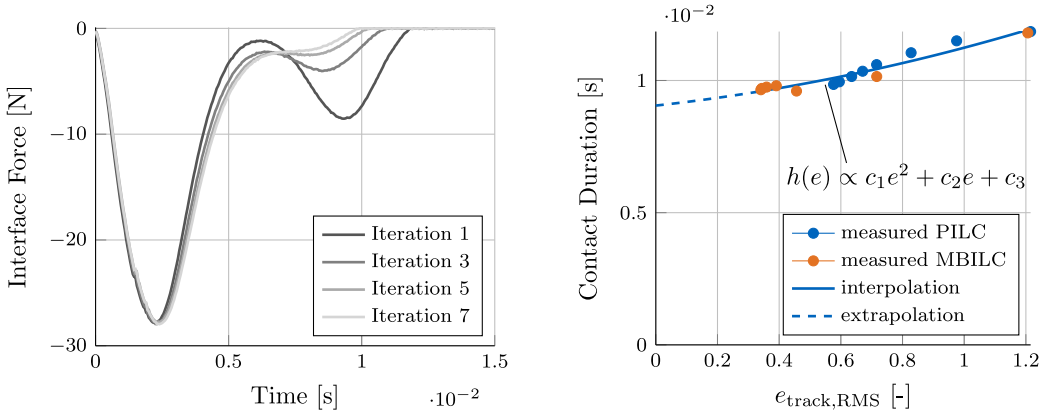


(a) The interaction force profile for different iterations for ILC learning with a proportional learning function.

(b) Measurements using P-type ILC and model-based ILC were used.

**Fig. 7.** FACE applied to the hybrid simulation of an impact: time history of the interface force and estimated contact duration $t_c$ using several iterations of the transfer system.

react quickly due to the rapid change in loading conditions by the impulse. Sensor miscalibration, noise, modeling errors, ... are not considered. Hence, also the relative RMS tracking error Eq. (1) is used to quantify $e$, which is evaluated using $\ddot{z}$ and $\ddot{z}'$ in this case. For this kind of RTHS testing, the shock phenomenon, which is the interaction, is of particular interest.

Since ILC is used to improve the tracking performance, the measured data during learning—with different values $e_{\text{track,RMS}}$—can be used as measurement points for the convergence plot. In contrast to Example 1, no arbitrary deterioration of the controller parameters or additional delay have to be implemented. The error $e_{\text{track,RMS}}$ is the largest in the first iteration. When ILC has converged, which means that the error has decreased and leveled off to its asymptotic value, the minimum achievable error $e_{\text{min}}$ is obtained. In the used setup, this was after seven iterations for both ILC implementations. Fig. 7(a) shows the interaction force profiles during different iterations: when the tracking due to ILC learning improves, the force profile changes and the contact duration $t_c$ decreases with improved actuator tracking. The contact duration is plotted for all iterations (with PILC and MBILC) in Fig. 7(b). To predict the reference solution, which is the contact duration when there was no tracking error $e_{\text{track,RMS}}$, a polynomial of degree two was fitted to the measurement points. The polynomial fit was then used to extrapolate to $e_{\text{track,RMS}} = 0$. After ILC learning, the contact duration at $e_{\text{min}}$ is $t_{\text{c,min}} = 9.65 \cdot 10^{-3}$ s and the predicted true contact duration is $t_{\text{c,pred}} = 9.05 \cdot 10^{-3}$ s. The estimated relative error is $\frac{t_{\text{c,min}} - t_{\text{c,pred}}}{t_{\text{c,pred}}} = 0.066$ and therefore suggests that the test was accurate in terms of replication of the contact duration. Since there is no reference solution available, the prediction accuracy of the FACE method cannot be validated here.

Fig. 7(a) also shows that the force profile exhibits a double-humped shape in the first iterations. The second force hump disappears for improved actuator tracking. If the peak values of the second force humps were plotted in a convergence plot for all iterations, one could see that there would not be a second force hump in case of perfect tracking. This is a unique feature of FACE: the visualization

of a QoI in the convergence plot (such as cf. Fig. 7(b)) helps to understand the influence of a certain error source on the investigated system dynamics.

### 4.3. Discussion

The work flow of the proposed FACE method, which was applied for the two application examples in this section, is summarized in Fig. 8.

The FACE method has several advantages compared to state-of-the-art assessment measures: Firstly, only data that are available during the test are required. The global influence of an error on the system dynamics can be investigated without requiring a system identification of any of the involved components. This makes it a method that is simple to implement and easy to apply. Furthermore, the parameters $q_{\text{min}}$ can be compared to $q_{\text{pred}}$ and the quantitative value can be easily compared and used for a decision whether the test succeeded or not. This is possible without the necessity for a reference solution. The results of the example applications suggest that a maximum relative error of 10% between $q_{\text{min}}$ and $q_{\text{pred}}$ can be used as acceptance criterion for the success of an RTHS test (sufficient fidelity). Further investigations are necessary, though, to confirm this threshold value.

For the successful application, an understanding of the main errors in the RTHS loop and of the QoIs is necessary. In our examples, the tracking error (denoted by actuator control error in Fig. 1) was the main error source, but the FACE method is not restricted to this. The application to other error sources presented in Fig. 1 could be as follows:

- Numerical time integration: The time step size or the integration algorithm can be varied and the RTHS results monitored. A convergence plot can be plotted for the variation of the time step size (quantity $e$) because the time integration is more accurate, the smaller the time step size.
- Sensor dynamics: The sensor dynamics could be quantified (error measure $e$) by taking the phase-error of the sensor at the fundamental frequency of the RTHS test. For example, the dynamic response of a force/torque sensor can be measured using an impact test (cf. [26]). To create the convergence plot for FACE, the measured data can be delayed by an additional delay.
- Communication/computational delays: Similar to the actuator/sensor dynamics, additional delay can be added in the communication to analyze the sensitivity of an RTHS setup to these delays.
- Sensor noise: To investigate the influence of sensor noise using the FACE method, additional Gaussian noise can be added to the signals. As the best measurement results if there is no noise, the standard deviation of the distribution could be the error measure $e$.

There are several error sources where it is tricky to find an appropriate measure $e$ that satisfies the condition that the reference dynamics results as $e \to 0$. In these cases, the FACE method offers an experimental sensitivity analysis, that is, the sensitivity of the RTHS setup to a certain error/uncertainty can be investigated. Then, no interpolation and extrapolation are performed. Examples are:

- Modeling errors: The system parameters of the modeled substructure can be changed to investigate the sensitivity of the RTHS setup to uncertain system parameters.
- Control–structure interaction (CSI): To change the dynamics of the actuator and thus the CSI, the controller parameters can be changed and the influence on the RTHS result monitored.[6]

Error sources that are out of the scope of the FACE method are sensor miscalibration, truncation due to A/D and D/A conversion and flexibility of the specimen support.

There can also be multiple error sources present in an RTHS setup. If only one of them is dominating the dynamics distortion of the RTHS test, the FACE method can be applied as presented before. Otherwise, the different error sources can for example be summarized within $e$ or a convergence plot is generated for each individual error. In the latter case, FACE can only be used as an experimental sensitivity analysis and not to predict the reference solution because there are still other sources of error in the loop. One has to be aware that the predicted value at $e = 0$ might still contain unquantifiable and probably even unknown errors. A further limitation is that the method assumes convergence towards $\hat{q}$. This implies the assumption that $e_{\text{min}}$ is small and that the dynamic behavior $e \in [0, e_{\text{min}}]$ does not change significantly, such that the interpolated relation $h(e)$ is also valid in this range. Future work will focus on how to determine whether $e_{\text{min}}$ is sufficiently small such that the estimate $q_{\text{pred}}$ can be trusted.

The application of the FACE method requires that the tests are repeatable and reproducible. Further requirements are that test execution is stable[7] and that the error source can be varied sufficiently before the test reaches the stability limit. Since test stability—and thus safe test execution—is jeopardized due to the additionally added errors, the control loop could be enhanced by a passivity controller to maintain test stability. A possible choice is Normalized Passivity Control (NPC), which monitors the power flow through the transfer system and dampens erroneously added energy by introducing a virtual damping force [33]. Note that when NPC is active, the measurement points should not be taken for the FACE method because the additional damping force distorts the RTHS results.

[6] The application of FACE to the RTHS Benchmark problem in [26] showed that FACE can be applied also if CSI is present. Nonetheless, this should be investigated in more detail in the future.

[7] According to the concept of passivity control, a test is unstable if the net energy flow from the transfer system to the dynamical system is larger than zero.

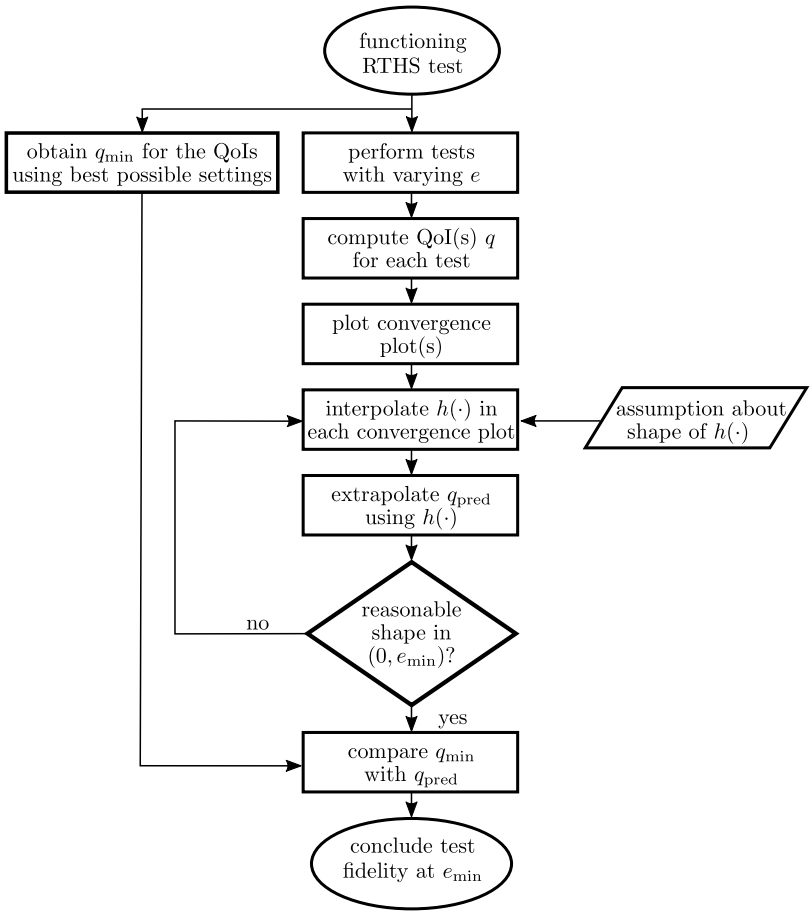


**Fig. 8.** Summary of the workflow in the FACE method.

Apart from the two application examples shown in this work, the FACE method has been applied to other linear and single degree of freedom systems in [26]. There, the FACE method is applied to the RTHS Benchmark system [34] and an RTHS test with contact. In the future, the FACE method will be applied to nonlinear systems as well. However, there will be limitations for highly nonlinear and chaotic systems because the functional course $e \in [0, e_{\min}]$ might be very different from the interpolated function $h(e)$.

## 5. Conclusion

Current quality assessment measures for RTHS have many disadvantages, including their difficult interpretation, the requirement of reference solutions or the need for a dynamics model of the experimental substructure and the transfer system. To circumvent them, Fidelity Assessment based on Convergence and Extrapolation (FACE) is proposed in this work. The underlying idea is to deliberately alter the amount of error in the RTHS loop and monitor the RTHS results to capture how sensitive the setup is to errors. The measurement points can be used to find a functional relation between the errors in the loop and the RTHS result. The functional relation, in turn, is further applied to predict the RTHS reference behavior. If all sources of error are included in the error measure, this corresponds to the reference solution. Two application examples were presented to showcase the applicability and the shortcomings of the FACE method: a virtual RTHS test, where also a reference solution is available, and a real RTHS test of a shock application. Different error measures and quantities of interest were used. Overall, the estimated reference was close to the real reference solution (deviations below 8 %). Furthermore, visualizing the sensitivity of an RTHS test in the convergence plot helped to understand the dynamic influence of errors on the RTHS results. This study reveals the benefits—such as the simple application, simple interpretation, the power to predict the reference solution accurately and the applicability to a large variety of systems—of the proposed FACE method. Also, the limitations of the current implementation were discussed, which include that the minimum achievable error must be close to the reference dynamics and must not change the underlying dynamics substantially in order to build an accurate prediction. Future research will consider more complex systems (including multiple degrees of freedom and nonlinear systems), a larger variety of error sources as well as diverse quantities of interest.

## Declaration of competing interest

The authors declare that they have no known competing financial interests or personal relationships that could have appeared to influence the work reported in this paper.

## Research data

The implementation of the FACE method for example application 1 (see Section 4.1) is available for download under the following link: https://gitlab.lrz.de/AM/rths.

## Acknowledgment

This research was funded by the Deutsche Forschungsgemeinschaft (DFG, German Research Foundation) with project number 450801414.

## References

[1] A.R. Plummer, Model-in-the-loop testing, Proc. Inst. Mech. Eng. I J. Syst. Control Eng. 220 (3) (2006) 183–199, http://dx.doi.org/10.1243/09596518JSCE207.
[2] X. Wang, R.E. Kim, O.-S.K. Kwon, I.-H. Yeo, J.-K. Ahn, Continuous real-time hybrid simulation method for structures subject to fire, J. Struct. Eng. 145 (12) (2019) http://dx.doi.org/10.1061/(ASCE)ST.1943-541X.0002436.
[3] V. Chabaud, Real-Time Hybrid Model Testing of Floating Wind Turbines (Ph.D. thesis), Norwegian University of Science and Technology, 2016.
[4] S. Olma, A. Kohlstedt, P. Traphöner, K.-P. Jäker, A. Trächtler, Observer-based nonlinear control strategies for hardware-in-the-loop simulations of multiaxial suspension test rigs, Mechatronics 50 (2018) 212–224.
[5] T. Sauder, S. Marelli, A. Sørensen, Probabilistic robust design of control systems for high-fidelity cyber–physical testing, Automatica 101 (2019) 111–119, http://dx.doi.org/10.1016/j.automatica.2018.11.040.
[6] G. Mosqueda, B. Stojadinović, S. Mahin, Implementation and Accuracy of Continuous Hybrid Simulation with Geographically Distributed Substructures, Earthquake Engineering Research Center, University of California, Berkeley, CA, USA, 2005.
[7] O. Mercan, J.M. Ricles, Stability and accuracy analysis of outer loop dynamics in real-time pseudodynamic testing of SDOF systems, Earthq. Eng. Struct. Dyn. 36 (11) (2007) 1523–1543, http://dx.doi.org/10.1002/eqe.701.
[8] A. Maghareh, S.J. Dyke, A. Prakash, G.B. Bunting, Establishing a predictive performance indicator for real-time hybrid simulation, Earthq. Eng. Struct. Dyn. 43 (15) (2014) 2299–2318, http://dx.doi.org/10.1002/eqe.2448.
[9] T. Ersal, R.B. Gillespie, M. Brudnak, J.L. Stein, H.K. Fathy, Effect of coupling point selection on distortion in internet-distributed hardware-in-the-loop simulation, in: Proceedings of the 2011 American Control Conference, 2011, pp. 3096–3103, http://dx.doi.org/10.1109/ACC.2011.5990934.
[10] T. Sauder, Fidelity of cyber-physical empirical methods, Exp. Tech. 44 (6) (2020) 669–685, http://dx.doi.org/10.1007/s40799-020-00372-x.
[11] C. Insam, D.J. Rixen, Fidelity assessment of real-time hybrid substructure testing: A review and the application of artificial neural networks, Exp. Tech. (2021) http://dx.doi.org/10.1007/s40799-021-00466-0.
[12] R.E. Christenson, S.J. Dyke, J. Zhang, G. Mosqueda, C. Chen, N. Nakata, P. Laplace, W. Song, Y. Chae, G. Marshall, G. Ou, C.A. Riascos Gonzales, C. Song, Hybrid Simulation: a Discussion of Current Assessment Measures, Technical Report, George E. Brown, Jr. Network for Earthquake Engineering Simulation (NEES), West Lafayette, In, 2014.
[13] A. Maghareh, S. Dyke, S. Rabieniaharatbar, A. Prakash, Predictive stability indicator: a novel approach to configuring a real-time hybrid simulation, Earthq. Eng. Struct. Dyn. 46 (1) (2017) 95–116, http://dx.doi.org/10.1002/eqe.2775.
[14] G. Mosqueda, B. Stojadinović, S. Mahin, Real-time error monitoring for hybrid simulation. Part 1: Methodology and experimental verification, J. Struct. Eng., ASCE 133 (2007) http://dx.doi.org/10.1061/(ASCE)0733-9445(2007)133:8(1100).
[15] C. Thewalt, M. Roman, Performance parameters for pseudodynamic tests, J. Struct. Eng. 120 (9) (1994) 2768–2781, http://dx.doi.org/10.1061/(ASCE)0733-9445(1994)120:9(2768).
[16] M. Wallace, D. Wagg, S. Neild, An adaptive polynomial based forward prediction algorithm for multi-actuator real-time dynamic substructuring, Proc. R. Soc. A Math. Phys. Eng. Sci. 461 (2005) 3807–3826.
[17] W. Xu, C. Chen, T. Guo, X. Yang, Reliability assessment of real-time hybrid simulation under worst-case scenarios using frequency-domain evaluation indices, Exp. Tech. 41 (2017) 237–249, http://dx.doi.org/10.1007/s40799-017-0172-7.
[18] T. Guo, C. Chen, W. Xu, F. Sanchez, A frequency response analysis approach for quantitative assessment of actuator tracking for real-time hybrid simulation, Smart Mater. Struct. 23 (4) (2014) http://dx.doi.org/10.1088/0964-1726/23/4/045042.
[19] G. Mosqueda, B. Stojadinović, S. Mahin, Real-time error monitoring for hybrid simulation. Part 2: Structural response modification due to errors, J. Struct. Eng., ASCE 133 (2007) http://dx.doi.org/10.1061/(ASCE)0733-9445(2007)133:8(1109).
[20] M. Ahmadizadeh, G. Mosqueda, Online energy-based error indicator for the assessment of numerical and experimental errors in a hybrid simulation, Eng. Struct. 31 (9) (2009) 1987–1996, http://dx.doi.org/10.1016/j.engstruct.2009.03.002.
[21] R. Botelho, R. Christenson, Robust stability and performance analysis for multi-actuator real-time hybrid substructuring, in: Dynamics of Coupled Structures, Vol. 4, 2015, pp. 1–7, http://dx.doi.org/10.1007/978-3-319-15209-7_1.
[22] R.M. Botelho, Real-Time Hybrid Substructuring for Marine Applications of Vibration Control and Structural Acoustics (Ph.D. thesis), University of Connecticut, 2015.
[23] G. Abbiati, S. Marelli, O. Bursi, B. Sudret, B. Stojadinović, Uncertainty propagation and global sensitivity analysis in hybrid simulation using polynomial chaos expansion, in: Proceedings of the Fourth International Conference on Soft Computing Technology in Civil, Structural and Environmental Engineering, Vol. 109, Civil-Comp Press, 2015, http://dx.doi.org/10.4203/ccp.109.23,
[24] G. Abbiati, Structural reliability analysis using deterministic hybrid simulations and adaptive kriging metamodeling, in: Proceedings of the 16th World Conference on Earthquake Engineering, 16WCEE, 2017.
[25] T. Sauder, Fidelity of Cyber-Physical Empirical Methods - Application to the Active Truncation of Slender Marine Structures (Ph.D. thesis), Norwegian University of Science and Technology, 2018.
[26] C. Insam, Fundamental Methods for Real-Time Hybrid Substructuring with Contact; Enabling Testing of Prosthetic Feet (Ph.D. thesis), Technical University of Munich, 2022.
[27] C. Insam, M.J. Harris, M.R. Stevens, R.E. Christenson, Real-time hybrid substructuring for shock applications considering effective actuator control, in: IMAC - Conference & Exposition on Structural Dynamics, 2022.

[28] C. Insam, M. Göldeli, T. Klotz, D.J. Rixen, Comparison of feedforward control schemes for real-time hybrid substructuring (RTHS), in: Dynamic Substructures, Vol. 4, Springer International Publishing, 2021, pp. 1–14.
[29] F. Chi, J. Wang, F. Jin, Delay-dependent stability and added damping of SDOF real-time dynamic hybrid testing, Earthq. Eng. Eng. Vib. 9 (3) (2010) 425–438, http://dx.doi.org/10.1007/s11803-010-0026-0.
[30] T. Horiuchi, M. Inoue, T. Konno, Y. Namita, Real-time hybrid experimental system with actuator delay compensation and its application to a piping system with energy absorber, Earthq. Eng. Struct. Dyn. 28 (10) (1999) 1121–1141, http://dx.doi.org/10.1002/(SICI)1096-9845(199910)28:10<1121::AID-EQE858>3.0.CO;2-O.
[31] P. Gawthrop, M. Wallace, S. Neild, D. Wagg, Robust real-time substructuring techniques for under-damped systems, Struct. Control Health Monit. 14 (4) (2007) 591–608, http://dx.doi.org/10.1002/stc.174.
[32] D. Bristow, M. Tharayil, A. Alleyne, A survey of iterative learning control: A learning-based method for high-performance tracking control, IEEE Control Syst. Mag. (2006) 96–114, http://dx.doi.org/10.1109/MCS.2006.1636313.
[33] C. Insam, A. Kist, H. Schwalm, D.J. Rixen, Robust and high fidelity real-time hybrid substructuring, Mech. Syst. Signal Process. 157 (2021) http://dx.doi.org/10.1016/j.ymssp.2021.107720.
[34] C.E. Silva, D. Gomez, A. Maghareh, S.J. Dyke, B.F. Spencer, Benchmark control problem for real-time hybrid simulation, Mech. Syst. Signal Process. 135 (2020) http://dx.doi.org/10.1016/j.ymssp.2019.106381.